



OPEN

Clinical characterization of respiratory large droplet production during common airway procedures using high-speed imaging

S. K. Mueller^{1✉}, R. Veltrup², B. Jakubaß², S. Kniesburges², M. J. Huebner⁴, J. S. Kempfle³, S. Dittrich⁴, H. Iro¹ & M. Döllinger²

During the COVID-19 pandemic, a significant number of healthcare workers have been infected with SARS-CoV-2. However, there remains little knowledge regarding large droplet dissemination during airway management procedures in real life settings. 12 different airway management procedures were investigated during routine clinical care. A high-speed video camera (1000 frames/second) was for imaging. Quantitative droplet characteristics as size, distance traveled, and velocity were computed. Droplets were detected in 8/12 procedures. The droplet trajectories could be divided into two distinctive patterns (type 1/2). Type 1 represented a ballistic trajectory with higher speed large droplets whereas type 2 represented a random trajectory of slower particles that persisted longer in air. The use of tracheal cannula filters reduced the amount of droplets. Respiratory droplet patterns generated during airway management procedures follow two distinctive trajectories based on the influence of aerodynamic forces. Speaking and coughing produce more droplets than non-invasive ventilation therapy confirming these behaviors as exposure risks. Even large droplets may exhibit patterns resembling the fluid dynamics smaller airborne aerosols that follow the airflow convectively and may place the healthcare provider at risk.

Abbreviations

ARDS	Acute respiratory distress syndrome
COVID-19	Coronavirus disease 2019
CPAP	Continuous positive airway pressure
FFP	Filtering face piece
FPS	Frames per second
LED	Light-emitting diode
MMAD	Mass median aerodynamic diameter
PEEP	Positive end-expiratory pressure
PPE	Personal protective equipment
Δp support	Pressure support ventilation
SARS-CoV-2	Severe acute respiratory syndrome coronavirus 2
WHO	World Health Organization

¹Department of Otolaryngology, Head and Neck Surgery, University Hospital Erlangen, Friedrich-Alexander-Universität Erlangen-Nürnberg (FAU), Waldstrasse 1, 91054 Erlangen, Germany. ²Laboratory for Computational Medicine, Department of Otolaryngology, Head and Neck Surgery, University Hospital Erlangen, Friedrich-Alexander-Universität Erlangen-Nürnberg (FAU), Erlangen, Germany. ³Department of Otolaryngology, Massachusetts Eye and Ear, Harvard Medical School, Boston, USA. ⁴Intensive Care Medicine/Department of Pediatric Cardiology, University Hospital Erlangen, Friedrich-Alexander-Universität Erlangen-Nürnberg (FAU), Erlangen, Germany. ✉email: mueller.sarinakatrin@gmail.com

Characteristics	n (%)
Mean age in years (\pm SD)	36.4 \pm 20.0
Gender	
Male	4/8 (50)
Female	4/8 (50)
Mean BMI (\pm SD)	25.4 \pm 8.8
Comorbidity	
COPD	3/8 (37.5)
Asthma	1/8 (12.5)
HNSCC	3/8 (37.5)
Heart condition	3/8 (37.5)

Table 1. Patient demographics including age, sex, BMI, and medical condition of all $n=8$ patients. HNSCC: head and neck squamous cell carcinoma.

The severe acute respiratory syndrome coronavirus 2 (SARS-CoV-2) leads to a high variability of symptoms. While some exhibit minor symptoms of an upper respiratory infection, some patients presents with severe sequelae similar to the acute respiratory distress syndrome (ARDS)^{1–3}. With worldwide dissemination of the disease and the increasing number of deaths, the modes of transmission in the healthcare environment is a subject of significant investigation^{4,5}. Many medical providers have been infected during the pandemic which in some cases has lead to death. It is therefore paramount to minimize healthcare worker exposure during highly “aerosolizing” procedures^{6,7}. Multiple recommendations to ensure maximal safety for the medical personnel during airway management procedures are being developed and regularly updated^{6–11}. This includes limiting some procedures to the minimum necessary, including non-invasive ventilation or tracheal cannula changes in SARS-CoV2 positive patients. Generally, aerosol transmission in the medical infectious disease community is described to occur by droplets (diameter $> 5 \mu\text{m}$)^{3,8,12} and airborne aerosols/ droplet nuclei (diameter $< 5 \mu\text{m}$)¹³. Aerosols are hereby defined as a suspension of solid or liquid particles in gas with particle size from 0.001 to over 100 μm ^{14,15}. Droplet nuclei are defined as the airborne residue of a potentially infectious (micro-organism bearing) aerosol from which most of the liquid has evaporated^{15,16}. However, this definition is an artificial construct and some authors suggested more detailed definitions (‘large-droplet’ diameter $> 60 \mu\text{m}$, ‘small droplet’ diameter $60 \mu\text{m}$ and ‘droplet nuclei’ diameter $< 10 \mu\text{m}$)¹⁵. Based on this definition, the current study will focus on analyzing large droplets.

Depending on size, these particles can be found in different anatomic parts of the upper and lower respiratory system^{17,18}. For SARS-CoV-2, there are already studies that have identified viable virus staying suspended within aerosols for hours hours^{18–20}. The number of detectable viruses following coughing versus exhaled breath has been studied intensively for other airborne disease and is currently under further investigation for SARS-CoV-2^{15,17,18,21,22}.

However, a precondition for an aerosol transmission is that the virus retains infectivity and replicability within these small particles. While it is controversially discussed if large droplets or aerosols contain a higher viral load and are responsible for viral transmission^{4,5,12,18,23}, there remains no quantitative data concerning the droplet trajectories and fluid patterns during airway management procedures in real life settings. In order to estimate the risk to medical personnel and to develop appropriate safety precautions it is important to analyze droplet size, aerodynamic characteristics and trajectories during different procedures. Therefore, the objective of this study was to assess the frequency, size and velocity of large respiratory droplets as well as characterize aerodynamic droplet patterns during common airway management procedures using high-speed imaging. The airway management procedures analyzed included non-invasive CPAP (continuous positive airway pressure) ventilation, high flow ventilation, tracheotomy cannula change, extubation, nebulizing and SARS-CoV-2 swab as well as common behavioral patterns including speaking and coughing.

Methods

Study design and inclusion of patients. All experiments were conducted at the Friedrich-Alexander-University Erlangen-Nürnberg. All experimental protocols as well as the study design were approved by the ethics committee of the Friedrich-Alexander-University Erlangen-Nürnberg (No 167_20B). Informed consent was obtained from all participants for participation in the study and for publication of identifying information/ images in an online open-access publication. All experiments and methods were performed in accordance with relevant guidelines and regulations. 12 different airway management procedures were investigated. A total of $n=8$ patients (6 males, 2 females) were included. The demographics are displayed in Table 1. Depending on the procedure, the individual scenarios were performed up to 5 times in different patients who medically required that procedure. All patients received the airway management procedures as part of their routine clinical care. None of these patients were infected with influenza or SARS-CoV-2.

Equipment, experimental setup and outcome measure. The patients were positioned in a routine posture. This included a supine position for the extubation and a seated for all remaining procedures. A sterile clean room was used for the experiments.

Our first outcome measure was to display droplets originating from the patients. The second outcome measure was to display droplets originating from the examiner wearing a FFP3 plus a surgical mask. For both outcome measures, the number of droplets, size, trajectories, distance travelled, and velocity were quantified.

To detect the droplets in the air, we developed a setup with light against a black background to record the scattered light with a high-speed camera. Two Fenix TK-35 LED lights were used to illuminate the scene in front of the patient (500 lumens each). The room as well as patient and examiner were covered in black clothing as background in order to display the illuminated particles as richly as possible. A high-end industrial high-speed camera Vision Research Phantom v2511 recorded the procedures. The camera was aimed perpendicular to the longitudinal axis of the patient at the height of head at a distance of 1.5 m. The recorded region was an area in front of the patient to represent the location where the provider would potentially stand during procedures, i.e. distance of up to 0.9 m in front of the patient. The videos were recorded at a spatial resolution of 1280×800 pixels yielding a minimal spatial resolution between $440 \mu\text{m}$ and $670 \mu\text{m}$ per pixel. This spatial limitation is caused by the choice of region (i.e. up to 0.9 m in horizontal direction to track the droplet trajectories) and the physical dimensions of the camera chip (5/3 inch). The recording rate was set to 1000 fps (frames per second) to accurately track the droplets. The camera control software PCC 2.6 was used. A reference image of a measuring rod was taken for subsequent metric computation of droplet trajectories.

Experimental conditions. The following common airway management procedures were studied:

1. Non-invasive CPAP with PEEP (positive end expiratory pressure) of 5 mbar, 6 mbar, 8 mbar and 10 mbar with and without coughing
2. Non-invasive CPAP with a PEEP of 5 mbar and a Δp support (pressure support ventilation) of 10 mbar, 15 mbar and 20 mbar with and without coughing
3. Non-invasive CPAP without leakage, with 50% leakage and with 80% leakage with and without coughing
4. Nasal oxygen via a nasal tube (Dahlhausen, Köln, Germany) at 2 l/min, 4 l/min, 6 l/min, 8 l/min and 10 l/min with and without coughing
5. High-flow nasal oxygen at 15 l/min without coughing
6. Nebulizing with an oxygen mask (Micro Mist Nebulizer plus mask, Hudson RCI, Wayne, PA, USA)
7. Tracheal cannula suctioning with (7.1) and without (7.2) filter (Hygroscopic Condenser Humidifier, Aqua + TS, Hudson RCI, Wayne, PA, USA)
8. Tracheal cannula removal without filter
9. Coughing and suctioning after tracheal cannula removal
10. Reinsertion of tracheal cannula without filter
11. Extubation (5.0 no cuff Vygon, Aachen, Germany)
12. SARS CoV-2 swab according to the WHO (World Health Organization) guidelines²⁴.

For procedure (1) to (3), a Dräger Evita V800 respirator (Lübeck, Germany) was used. For procedures (7) to (10), a Tracheoflex, 9,0 mm, with Cuff (Rüsch, Berlin, Germany) was applied. The nebulizing therapy was used for representation of fine particle aerosols (manufacturer's information mass median aerodynamic diameter (MMAD) $3.6 \mu\text{m}$).

Additionally, the procedure speaking "stay healthy" was used as positive control (13).

Image processing and quantification techniques. A software script specially designed for evaluating the recorded video data was implemented in MATLAB. It allows the manual tracking and computes the size of particles. Droplet sizes were found to be between 1 and 4 pixels. Based on the physical specification of the camera chip, detected particles were divided into three categories, large ($1000 < d < 2000 \mu\text{m}$), medium ($670 \mu\text{m} < d \leq 1000 \mu\text{m}$) and small ($d \leq 670 \mu\text{m}$). In the following, we refer to this size distribution when speaking of small, medium, or large droplets. Traveled distances and velocity values of the particles were computed.

Results

Characterization of two main trajectory patterns. All visible droplets were tracked in each condition. No droplets were visible for procedures 3, 5, 6, 11, 12. For procedures 1, 2, 7.2, 8, and 9 all visible droplets were tracked. For procedures 4, 7.1, 10 and 13 the number of droplets exceeded the ability for individual tracking. Comparing all scenarios, two major droplet trajectories were discerned.

Type 1 represented a ballistic curve that descended in a predictable curve with a maximal velocity of 26.41 m/s. The velocity was maximal at start and exponentially decelerated over time to a minimal velocity of 0.04 m/s. The maximal distance travelled in horizontal x-direction was 0.73 m and in upper vertical y-direction 0.14 m. The average diameter of the droplets was $0.66 \text{ mm} \pm 0.32 \text{ mm}$. A procedure with type 1 was e.g. 13 speaking "stay healthy" (Fig. 1A,B).

Type 2 was unordered and non-directed. These droplets were mainly driven by convective flow within the ambient air with random acceleration and deceleration over time similar to the behavior expected by aerosols $< 5 \mu\text{m}$. The minimal velocity was 0.01 m/s and the maximal velocity was 7.02 m/s. The maximal distance travelled in horizontal direction was 0.70 m and 0.16 m in the upper vertical direction. Each droplet showed a different movement pattern. The average size of the droplets was again $0.66 \text{ mm} \pm 0.16 \text{ mm}$. A procedure with type 2 was e.g. 10 reinsertion of the cannula (Fig. 1C,D).

For all conditions that showed a type 1 pattern, there was also a type 2 pattern seen. This included all conditions (4, 7.1, 9, and 13) where coughing or speaking was performed (Fig. 1E,F; video 1). For procedure 4, 7.1, 9, and 13, small ($60 < d \leq 670 \mu\text{m}$) to large ($1000 < d < 2000 \mu\text{m}$) droplet sizes were seen. Comparing the two patterns,

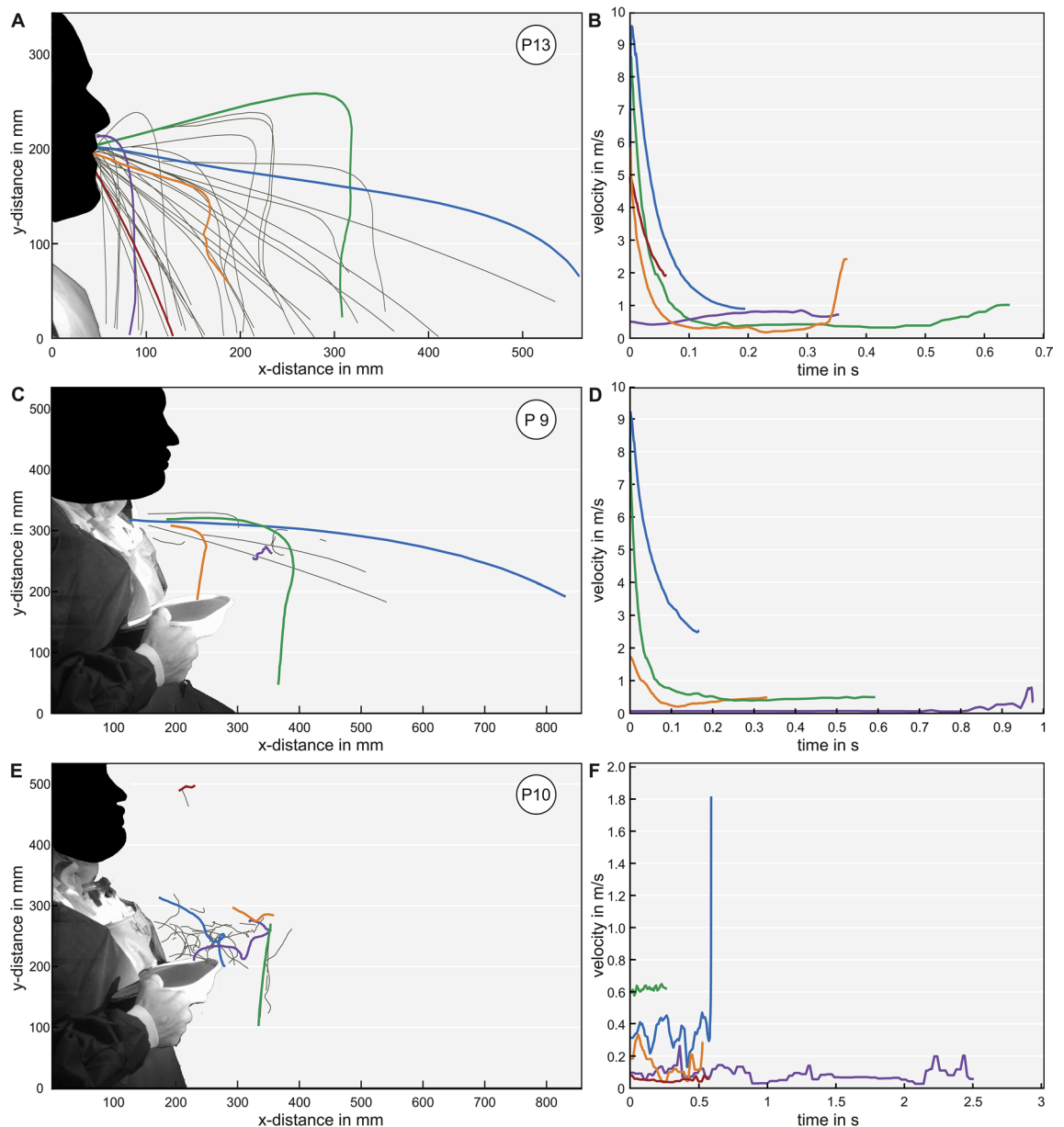


Figure 1. Examples of computed trajectories (left) and velocities (right) for tracked droplets within three conditions. The most representative trajectories were selected. The colored trajectories correspond to the matching velocity color: (A) Droplet trajectories for the positive control speaking “stay healthy” (type 1 > type 2) (B) Velocity–time diagram for speaking “stay healthy” (C) Droplet trajectories for coughing out of the tracheostomy without tracheal cannula (type 2 > type 1) (D) Velocity–time diagram for coughing out of the tracheostomy without tracheal cannula (E) Droplet trajectories for the insertion of a tracheal cannula without a filter (type 2) (F) Velocity–time diagram for the insertion of a tracheal cannula without filter.

type 2 droplets remained in the air after type 1 already descended. However, for the conditions 1, 2, 7.2, 8 and 10 (non-invasive ventilation, tracheal cannula removal and reinsertion) only a type 2 pattern was seen. For conditions 1, 2, 7.2, and 10, only small droplet sizes were seen. For condition 8, there was also a large droplet size. For conditions 3, 5, 6, 11 and 12, no droplets could be seen (Fig. 2A, B).

Reduction in droplet amount using a filter during tracheal cannula suctioning. Comparing tracheal cannula suctioning with and without filter, significant differences were seen. In the scenario without a filter (procedure 7.1), there was a large amount of droplets with non-directed trajectories (type 2). With a filter (procedure 7.2) there was an average 80% reduction in the amount of droplets with type 2 behavior (Fig. 3A,B).

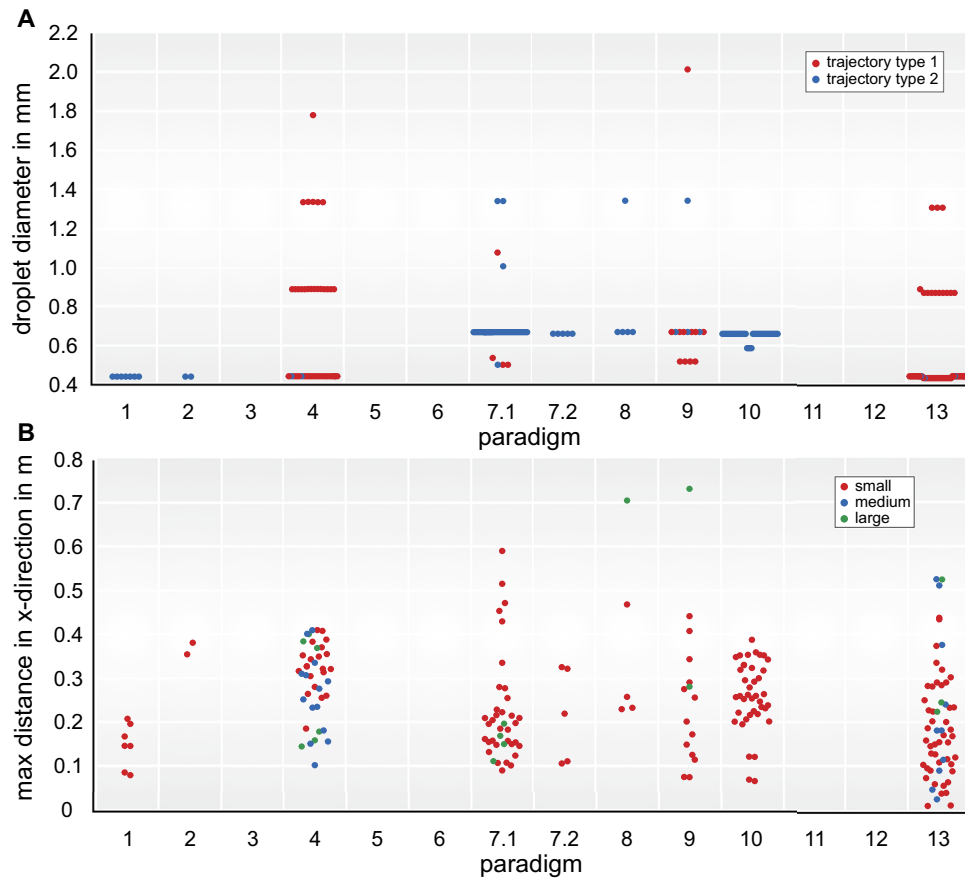


Figure 2. (A) Beeswarm diagrams over all 13 procedures representing (A) the droplet size separated for trajectory types and (B) the maximal distance travelled in horizontal x direction separated for the three droplet sizes. For (A) the red color represents type 1 and the blue color type 2. For (B) the red color represents small droplets, the blue color medium sized droplets and the green color large droplets.

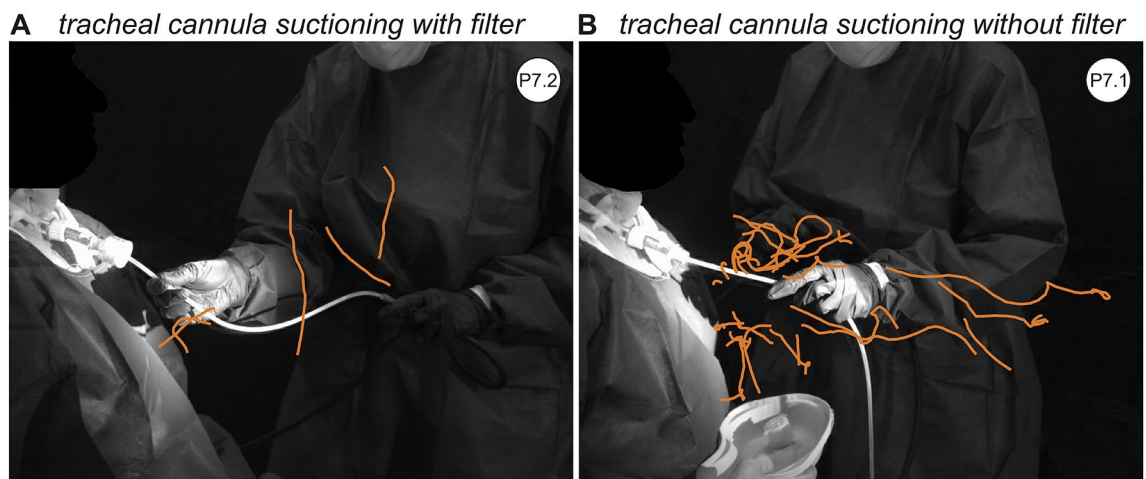


Figure 3. High-speed camera image representing the trajectories of tracheal cannula suction (A) with and (B) without a filter. The orange lines represent the droplet trajectories.

After removal of the filter, many droplets were visible and could be characterized as type 2 trajectories. In case of coughing after removal or insertion of the tracheal cannula, the droplet formation increased and changed to a combined type 1 and 2 pattern.

Procedure	(# video)	(# tracked)	# size			# trajRating		v_{max} (m/s)		v_{min} (m/s)		x_{max} (m)		$dist_{max}$ (m)		y_{max} (m)	
			S	m	l	t1	t2	t1	t2	t1	t2	t1	t2	t1	t2	t1	t2
1	(1)	7	7	–	–	–	7	–	0.36	–	0.02	–	0.21	–	0.30	–	0.16
2	(1)	2	2	–	–	–	2	–	0.11	–	0.01	–	0.38	–	0.21	–	0.00
4	(2)	40	20	14	6	38	2	26.41	4.41	0.50	0.11	0.41	0.31	0.56	0.34	0.14	0.06
7.1	(3)	38	–	34	4	4	34	0.59	7.02	0.04	0.02	0.19	0.59	0.08	0.33	0.10	0.10
7.2	(1)	5	–	5	–	–	5	–	0.33	–	0.04	–	0.32	–	0.18	–	0.10
8	(1)	5	–	4	1	–	5	–	0.45	–	0.01	–	0.70	–	0.13	–	0.00
9	(2)	15	–	13	2	11	4	21.69	2.35	0.12	0.01	0.73	0.28	0.73	0.06	0.08	0.01
10	(2)	39	–	39	–	–	39	–	1.86	–	0.01	–	0.39	–	0.12	–	0.12
13	(2)	58	45	10	3	53	5	10.40	4.21	0.17	0.15	0.52	0.22	0.55	0.37	0.06	0.04

Table 2. Conditions, number of recordings, number of recordings where droplets were visible, droplet sizes, trajectory types and computed quantities. The five conditions not provided (i.e. 3, 5, 6, 11, 12) did not show any visible droplets.

Speaking and coughing produce more droplets than non-invasive ventilation. Our positive control “stay healthy” as well as coughing showed the highest number (tracking number $n=58$) of droplets (video 2). In terms of coughing, this is true both for coughing through the mouth without a tracheostomy as well as coughing through the tracheostomy opening. Coughing through the mouth demonstrated the fastest velocities with 26.41 m/s.

In contrast, of all non-invasive CPAP procedures and oxygen delivery via a nasal tube only a few scenarios showed droplets. These scenarios included CPAP with PEEP at 10 mbar and CPAP with PEEP of 5 mbar with a Δp support of 10 mbar (procedures 1 and 2). Low-flow and high-flow of oxygen (2–15 l, procedures 4 and 5) showed no droplets without coughing. However, coughing during nasal oxygen flow generated a large amount of droplets. Here, the amount of droplets was highest during the first cough and decreased for subsequent coughs.

Sampling a SARS-CoV-2 swab according to the WHO guidelines demonstrated a similar effect²⁴. During the sampling itself, no droplets could be seen (procedure 12). However, droplets were detected if the patient spoke or coughed during or after the procedure. During extubation, no coughing and no droplets were visible. At the end of the tracheal tube, gummy secretions were seen (procedure 11). During nebulization, fine aerosols (manufacturer’s information MMAD 3.6 μm) could be detected using our method. However, aerosols could not be quantified due to their abundance. All results are displayed in Table 2.

FFP3 mask plus surgical mask prevents spread of droplets. We analyzed simultaneously how many droplets originated from the examiner at the same sequences. Although the examiner spoke nearly constantly during the entire procedures, to instruct or calm down the patient, no droplets were seen at any time.

Discussion

During the COVID-19 pandemic, several studies have emphasized the concept of aerosolized transmission of the virus. SARS-CoV-2 positive aerosols down to a size of 4 μm and below were shown to contain contagious viral particles²⁵. Around 450,000 health care workers are estimated to have been infected up to this time point and an appalling number have died²⁶. As a result, several routine airway management procedures are currently being adapted or avoided in SARS-CoV-2 positive patients. This is the first study to evaluate common airway management procedures performed in real-life patients in order to characterize droplet patterns.

We applied high-speed imaging to visualize droplets in the region of interest (entire dispersion of droplets). For our study, we performed the airway management procedures as realistically as possible on patients. We focused on larger respiratory droplets rather than on airborne aerosols (smaller than 5 μm) due to the suspected higher viral load^{21,22}. In our results, two different trajectory patterns of the droplets emerged which we categorized as type 1 and 2. All droplet sizes are found in both trajectory types: type 1 (i.e. classic ballistic trajectory) and type 2 (i.e. driven by convective forces of the air resulting from the air management procedure itself). Due to the low mass of the droplets, convective lifting forces balance with their gravitational forces resulting in a floating behavior similar to much smaller aerosols. This results in a non-predictive, complex, trajectory pattern, alternating accelerations and decelerations capable of reaching the provider’s face. To the best of our knowledge, this behavior has not been described for such large droplets during these air management procedures in patients before. We could show that the droplets described in type 2 remained in the air for a minimum of 7 s. With an average human being roughly breathing every 5 s (12/min), we suggest that the droplets persist long enough for another person to inhale. We hypothesize that by remaining longer in the air and recirculating non-predictively, type 2 droplets are more dangerous for disease transmission than type 1 droplets. Importantly, our type 2 pattern is similar to previously described aerodynamic patterns of fine aerosols (<5 μm) although droplets were significantly larger^{27,28}. This again underlines that the cut-off value that defines how particles behave is not necessarily bound to size. On the contrary, in certain real life situations like the airway management procedures that create a distinctive air flow itself, even larger droplets do not follow ballistic patterns but are able to float in the air longer than expected. This also underlines the recommendation to reduce the number of personnel to a

minimum necessary^{29,30}. Whether larger droplets or fine particle aerosols with the same aerodynamic pattern are more contagious remains to be verified in virological experiments.

Our results also confirm that the usage of a filter significantly reduced the amount of droplets in comparison to a non-occluded tracheal cannula during tracheal cannula suctioning. Additionally, we could not detect any droplets originating from the examiner who was wearing the combination of a FFP3 and a surgical mask. The same examiner, however, had shown a droplet formation during the positive control “stay healthy” without a mask. Various international guidelines recommend the use of a viral filter e.g. in combination with a heat-moisture exchanger during intubation and extubation^{31–34}. A previous study of our group showed significant reduction of droplets during tracheal cannula procedures using a filter³⁵. However, the filter did not avoid droplet spread completely which leaves health care workers still at risk. Additionally, the use of combination of a FFP3 and a surgical mask as source control is generally assumed to be one of the most important measures to prevent airborne virus transmission³⁶. There has been extensive research on the benefits of wearing masks and our data underline those results^{18,28,29,37}.

Furthermore, our results show that speaking and coughing produced the highest amount of droplets with the highest velocities. In previous research³⁸, the sentence “stay healthy” was shown to produce speech associated droplets. Our study confirmed that coughing and speaking produced the largest amount of droplets over all conditions. Coughing demonstrated the highest velocity measurements and the furthest distance travelled. Our velocity during coughing was even higher than reported in previous studies³⁹. With respect to particle numbers, speaking and coughing produced significant more droplets than routine airway management procedures including CPAP non-invasive ventilation, high-flow oxygen administration using a nasal cannula and extubation. As recommended in literature^{7,9,40}, in a highly sedated, ventilated patient with a blocked cuff at either breathing tube or tracheal cannula and an intercalated viral filter, droplet formation is minimal. Our results show that even non-invasive ventilation in a breathing patient shows minimal droplet concentration. However, the awake patient that is able to cough and speak appears to be the most dangerous. As a patient on non-invasive CPAP or nasal cannula ventilation is awake, the patient is potentially able to cough and speak which represents a potential risk. These findings underlie the unconditional need of personal protective equipment (PPE). Summarizing, our results show that aerodynamic measurements during airway management procedures are able to provide valuable information for the safety of the medical personnel and for the patients.

It is also important to address limitations of the study. Although no detected type 2 particle left the field of view in horizontal as well as vertical direction, type 2 particles showed aerosol behavior i.e. hovering in the air and commonly following convective flows in the environment. As a consequence, we cannot exclude that type 2 particles are able to convectively travel over larger distances than those measured in our experiments. Due the physical limitations of the camera chip and the large region of interest, we were only able to quantify larger droplets (> 60 µm) and were not able to quantify small droplets / aerosols that did not illuminate camera-pixels enough to stand out against the black background. Therefore, it is important to mention that in those airway management procedures where we could not detect any droplets, the simultaneous generation of fine particle aerosols cannot be excluded. In fact, previous studies have shown that fine particle aerosols are generated and that e.g. talking predominantly produces fine diameter particles (< 5 µm)^{41–43}. Hence, the generation of fine particle aerosols during airway management procedures has to be investigated in further studies.

Conclusions

Respiratory large droplet patterns generated during airway management procedures follow two trajectories, one ballistic, and one approximating that of smaller airborne particles following a random convective pattern. Speaking and coughing produced both a larger amount and higher velocity droplets as compared to the investigated airway management procedures. Facial masks significantly reduced droplet dissemination as did the use of a tracheal cannula filter.

Received: 27 June 2020; Accepted: 22 April 2021

Published online: 20 May 2021

References

1. Lescure, F. *et al.* Clinical and virological data of the first cases of COVID-19 in Europe: a case series. *Lancet Infect. Dis.* **20**, 697–706 (2020).
2. Weiss, P. & Murdoch, D. Clinical course and mortality risk of severe COVID-19. *Lancet* **395**, 1014–1015 (2020).
3. Wolfel, R. *et al.* Virological assessment of hospitalized patients with COVID-2019. *Nature* **581**, 465–469 (2020).
4. Liu, J. *et al.* Community transmission of severe acute respiratory syndrome coronavirus 2. *Emerg. Infect. Dis.* **26**, 1320–1323 (2020).
5. Li, Q. *et al.* Early transmission dynamics in Wuhan, China, of novel coronavirus-infected pneumonia. *N. Engl. J. Med.* **382**, 1199–1207 (2020).
6. Matava, C., Yu, J. & Denning, S. Clear plastic drapes may be effective at limiting aerosolization and droplet spray during extubation: implications for COVID-19. *Can. J. Anaesth* **67**, 902–904 (2020).
7. Tay, J., Khoo, M. & Loh, W. Surgical considerations for tracheostomy during the COVID-19 pandemic: lessons learned from the severe acute respiratory syndrome outbreak. *JAMA Otolaryngol. Head Neck Surg.* **146**, 517–518 (2020).
8. Wang, J. & Du, G. COVID-19 may transmit through aerosol. *Irish J. Med. Sci* **24**, 1–2 (2020).
9. Lindemann, J. *et al.* Chirurgische Aspekte zur Tracheostomie bei COVID-19-positiven Patienten - Stellungnahme im Auftrag der Deutschen Gesellschaft für HNO-Heilkunde, Kopf- und Halschirurgie (DGHNO-KHC) und der AG Laryngologie & Trachealerkrankungen. *Laryngorhinootologie* **99**, 282–284 (2020).
10. Aziz, S. *et al.* Managing ICU surge during the COVID - 19 crisis : rapid guidelines. *Intensive Care Med.* **46**, 1303–1325 (2020).
11. Arabi, Y. M., Murthy, S. & Webb, S. What’s new in intensive care COVID-19: a novel coronavirus and a novel challenge for critical care. *Intensive Care Med.* **46**, 833–836 (2020).

12. Modes of transmission of virus causing COVID-19: implications for IPC precaution recommendations. <https://www.who.int/news-room/commentaries/detail/modes-of-transmission-of-virus-causing-covid-19-implications-for-ipc-precaution-recommendations>. S. B. 29 M. 2020. World Health Organization (2020)
13. Milton, D. K. A Rosetta Stone for understanding infectious drops and aerosols. *J. Pediatr. Infect. Dis. Soc.* <https://doi.org/10.1093/jpids/piaa079> (2020).
14. Hinds, W. *Aerosol Technology* (John Wiley Sons, New York, 1982).
15. Tang, J., Li, Y., Eames, C., Chan, P. & Ridgway, G. L. Factors involved in the aerosol transmission of infection and control of ventilation in healthcare premises. *J. Hosp. Infect.* **64**, 100–114 (2006).
16. Wells, W. On air-borne infection. II. Droplets and droplet nuclei. *Am. J. Hyg.* **20**, 611–618 (1934).
17. Tellier, R., Li, Y., Cowling, B. & Tang, J. Recognition of aerosol transmission of infectious agents: a commentary. *BMC Infect. Dis.* **19**, 101 (2019).
18. Fennelly, K. P. Particle sizes of infectious aerosols : implications for infection control. *Lancet Respir.* **2600**, 1–11 (2020).
19. van Doremalen, N. *et al.* Aerosol and surface stability of SARS-CoV-2 as compared with SARS-CoV-1. *N Engl J Med* **382**, 1564–1567 (2020).
20. Santarpia, J. *et al.* Transmission potential of SARS-CoV-2 in viral shedding observed at the university of nebraska medical center. *Sci. Rep.* **10**, 12732 (2020).
21. Johnson, G. & Morawska, L. The mechanism of breath aerosol formation. *J. Aerosol. Med. Pulm. Drug Deliv.* **22**, 229–237 (2009).
22. Workman, A. *et al.* Endonasal instrumentation and aerosolization risk in the era of COVID-19: simulation, literature review, and proposed mitigation strategies. *Int. Forum Allergy Rhinol.* **10**, 798–805 (2020).
23. Huang, C. *et al.* Clinical features of patients infected with 2019 novel coronavirus in Wuhan, China. *Lancet* **95**, 497–506 (2020).
24. Laboratory testing for 2019 novel coronavirus (2019-nCoV) in suspected human cases. Interim guidance. WHO/COVID-19/laboratory/2020.5. World Health Organization, Geneva, Switzerland. <https://www.who.int/publication>.
25. Chia, P. *et al.* Detection of air and surface contamination by severe acute respiratory syndrome coronavirus 2 (SARS-CoV-2) in hospital rooms of infected patients. *Nat. Commun.* **11**, 2800 (2020). <https://www.cbc.ca/news/health/icn-nurses-covid-deaths-1.5596300>. accessed 06/06/2020
26. Knight, V. Viruses as agents of airborne contagion. *Ann. N. Y. Acad. Sci.* **353**, 147–156 (1980).
27. Prather, B. K. A., Wang, C. C. & Schooley, R. T. Reducing transmission of SARS-CoV-2. *Science* **368**(6498), 1422–1424 (2020).
28. Morawska, L. *et al.* How can airborne transmission of COVID-19 indoors be minimised?. *Environ. Int.* **142**, 105832 (2020).
29. Morawska, K. & Milton, D. It is time to address airborne transmission of COVID-19. *Clin Infect Dis* <https://doi.org/10.1093/cid/ciaa939> (2020).
30. <https://sccm.org/SurvivingSepsisCampaign/Guidelines/COVID-19>. accessed 06/06/2020
31. <https://canadiem.org/recommendations-for-covid-19-intubation-an-infographic/>. accessed 06/06/2020
32. Luo, M. *et al.* Precautions for intubating patients with COVID-19. *Anesthesiology* **132**, 1616–1618 (2020).
33. Silva, D. F. D., McCulloch, T. J., Lim, J. S., Smith, S. S. & Carayannis, D. Extubation of patients with COVID-19. *Br. J. Anaesth.* **125**, e192–e195 (2020).
34. Kempfle, J., Löwenheim, H., Huebner, M., Iro, H. & Mueller, S. Management of COVID-19 patients with tracheostomy: Review of literature and demonstration. *HNO* **1–10** (2020).
35. Organización Mundial de la Salud. Advice on the use of masks in the context of COVID-19: interim guidance-2. *Guía Interna la OMS* 1–5 (2020). doi:<https://doi.org/10.1093/jiaa077>
36. Morawska, L. & Cao, J. Airborne transmission of SARS-CoV-2: the world should face the reality. *Environ. Int.* **139**, 105730 (2020).
37. Anfinrud, P., Stadnytskyi, V., Bax, C. & Bax, A. Visualizing speech-generated oral fluid droplets with laser light scattering. *N. Engl. J. Med.* **382**, 2061–2063 (2022).
38. Tang, J. & Settles, G. Coughing and aerosols. *N. Engl. J. Med.* **359**, e19 (2008).
39. Wax, R. S. & Christian, M. D. Practical recommendations for critical care and anesthesiology teams caring for novel coronavirus (2019-nCoV) patients. *Can. J. Anesth.* **67**, 568–576 (2020).
40. Yan, J. *et al.* Infectious virus in exhaled breath of symptomatic seasonal influenza cases from a college community. *PNAS* **115**, 1081–1086 (2018).
41. Milton, D., Fabian, M., Cowling, B., Grantham, M. & McDevitt, J. Influenza virus aerosols in human exhaled breath: particle size, culturability, and effect of surgical masks. *PLOS Pathog.* **9**, e1003205 (2013).
42. Asadi, S. *et al.* Aerosol emission and superemission during human speech increase with voice loudness. *Sci. Rep.* **9**, 2349 (2019).

Author contributions

S.K.M., R.V., M.J.H. performed the experiments. S.K.M., R.V., B.J., S.K., M.D., J.S.K. and H.I. analyzed the data. S.K.M. drafted the manuscript. S.K.M., R.V., B.J., S.K., M.D., J.S.K., S.D. and H.I. helped with the revision. All authors edited the manuscript.

Funding

This research did not receive any specific grant from funding agencies in the public, commercial, or not-for-profit sector. Open Access funding enabled and organized by Projekt DEAL.

Competing interests

The authors declare no competing interests.

Additional information

Supplementary Information The online version contains supplementary material available at <https://doi.org/10.1038/s41598-021-89760-w>.

Correspondence and requests for materials should be addressed to S.K.M.

Reprints and permissions information is available at www.nature.com/reprints.

Publisher's note Springer Nature remains neutral with regard to jurisdictional claims in published maps and institutional affiliations.



Open Access This article is licensed under a Creative Commons Attribution 4.0 International License, which permits use, sharing, adaptation, distribution and reproduction in any medium or format, as long as you give appropriate credit to the original author(s) and the source, provide a link to the Creative Commons licence, and indicate if changes were made. The images or other third party material in this article are included in the article's Creative Commons licence, unless indicated otherwise in a credit line to the material. If material is not included in the article's Creative Commons licence and your intended use is not permitted by statutory regulation or exceeds the permitted use, you will need to obtain permission directly from the copyright holder. To view a copy of this licence, visit <http://creativecommons.org/licenses/by/4.0/>.

© The Author(s) 2021, corrected publication 2021